Metallodrugs as protein modulators

Batista de Almeida, Andreia Filipa

B1. Gold(I) Organometallic Compounds with Biological Activity in Cancer Cells

This chapter is published:

Benoit Bertrand*, Andreia de Almeida*, Evelien P.M. van der Burgt, Michel Picquet, Anna Citta, Alessandra Folda, Maria Pia Rigobello, Pierre Le Gendre, Ewen Bodio and Angela Casini

New Gold(I) Organometallic Compounds with Biological Activity in Cancer Cells

Eur.J.Inorgn.Chem. (2014) 27:4532-4536

Supplementary information available: 10.1002/ejic.201402248

*Authors contributed equally to this work

Abstract

N-Heterocyclic carbene gold(I) complexes bearing a fluorescent coumarin ligand were synthesized and characterized by various techniques. The compounds were examined for their antiproliferative effects in normal and tumor cells *in vitro*; they demonstrated moderate activity and a certain degree of selectivity. The compounds were also shown to efficiently inhibit the selenoenzyme thioredoxin reductase (TrxR), whereas they were poorly effective towards the glutathione reductase (GR) and glutathione peroxidase enzymes. Notably, {3-[(7-methoxy-2-oxo-*2H*-chromen-4-yl)methyl]-1-methylimidazol-2-ylidene}(tetra-O-acetyl-1-thio-β-d-glucopyranosido)gold(I) (3) showed a pronounced inhibition of TrxR also in cell extracts, and it appeared to activate GR. Mechanistic information on the system derived from biotin-conjugated iodoacetamide assays showed selective metal binding to selenocysteine residues. Preliminary confocal fluorescence microscopy experiments proved that **3** enters tumor cells, where it reaches the nuclear compartment.

1.1. Introduction

Following the clinical success of cisplatin, many platinum and non-platinum metallodrugs are currently investigated as experimental antitumor agents with different mechanisms of action and improved pharmacological properties with respect to existing drugs [1]. However, major challenges must be faced to reach such a goal, including the identification of the actual biological targets for metal compounds, as well as the determination of their distribution in tissues, cells and subcellular compartments, to achieve an understanding of the possible mechanisms of biological activity [2].

It is worth mentioning that gold complexes belonging to various families have drawn attention in the last years as new generation of experimental anticancer agents, and have shown to possess anticancer properties *in vitro* and *in vivo* [3, 4]. Notably, various organometallic gold complexes were synthesized in which the presence of a direct carbon-gold bond greatly stabilizes the gold oxidation state and guarantees more controlled chemical speciation in biological systems. In general, both organometallic gold(I) and gold(III) compounds have increased stability compared to the classical gold-based coordination complexes, allowing to design compounds in which the redox properties and ligand exchange reactions can be modulated to achieve selective activation in diseased cells.

Mechanistic studies showed that interactions of gold complexes with DNA are not as tight as found for platinum(II) drugs, suggesting the occurrence of different pathways to cytotoxicity [5-7]. Indeed, several studies supported the idea that mitochondria and pathways of oxidative phosphorylation are among the primary intracellular targets [8]. Moreover, inhibition of the seleno-enzyme thioredoxin reductase (TrxR) appears as a common mechanistic trait to explain (at least partially) the cytotoxic actions of gold complexes, as strong TrxR inhibition may eventually lead to apoptosis through a mitochondrial pathway [9, 10]. TrxRs are large homodimeric proteins playing a crucial role in the intracellular redox balance [11]. Two major isoforms are known, a cytosolic (TrxR1) and a mitochondrial one (TrxR2); their main function is the reduction of 12 kDa disulfide protein thioredoxin (Trx) to its dithiolic form [9]. Interestingly, the view that TrxRs are

effective "druggable" targets for inorganic compounds is supported, for example, by mechanistic investigation of arsenic trioxide, a potent TrxR inhibitor now approved for promyelocytic leukaemia treatment [12].

Within this frame, in the last years, gold(I) N-heterocyclic carbenes (NHCs) have transformed from niche compounds to some of the most popular scaffolds in medicinal inorganic chemistry [13, 14]. For example, studies by our group, et al., confirmed that many gold(I) NHC complexes with the 1,3-substituted imidazol-2-ylidene and benzimidazol-2-ylidene ligands of the type NHC-Au-L (L = Cl or 2-mercapto-pyrimidine) can potently inhibit both of the cytosolic and mitochondrial isoforms of the TrxR enzyme [15]. The compounds showed potent and selective TrxR inhibition properties in particular in cancer cell lines.

On the basis of these promising results, we report here on the synthesis and characterization of three new gold(I) NHC complexes bearing a coumarin moiety. This functionalization was chosen because coumarin derivatives are one of the most studied fluorophore for *in vitro* imaging. They display a good chemical and photochemical stability, relatively high absorption coefficients and quantum yields, and are very easily available. Moreover, two of the new derivatives bear 1-thio-β-D-glucose-type ligands, which may affect the uptake of the compounds as previously observed for other gold(I) complexes [16].

All compounds were tested *in vitro* against different human cancerous cell lines (i.e. A2780, MCF7, and A549) along with non-cancerous cells (i.e. HEK-293T). To gain preliminary mechanistic insights, we screened the interactions of compounds 1–4 with TrxR. The compounds were also screened for inhibition of glutathione reductase (GR), a pyridine disulfide oxidoreductase able to maintain glutathione in its reduced state, as well as of the seleno-enzyme glutathione peroxidase (Gpx). Additional complementary information regarding the enzyme metallation process and possible binding sites was obtained through the application of a specific biochemical assay that relies on the thiol-tagging reagent, BIAM (biotin-conjugated iodoacetamide). Furthermore, fluorescence confocal microscopy has been used to study compounds' uptake in cancer cells.

1.2. Results and Discussion

1.2.1. Synthesis

The chlorido gold carbene was efficiently synthesized in three steps by adapting literature procedures (Scheme 1) [17, 18]. Thus, 1-methylimidazole was alkylated by the commercially available 4-bromomethyl-7-methoxycoumarin to obtain the imidazolium salt **1** in 95% yield. Afterwards, **1** was treated with silver oxide at room temperature in the dark to generate the silver carbene which was transferred to gold by reaction with the precursor [AuCl(tht)]. The formation of the gold carbene complex **2** was assessed by ^{1}H and $^{13}C\{^{1}H\}$ NMR spectroscopy. The singlet corresponding to the imidazolium proton disappeared and a significant shift of the signal of the C-2 carbon was observed going from 138.2 ppm in the imidazolium salt to 173.5 ppm in the complex (carbenic carbon). This behaviour is in agreement with already reported data in the literature ([19] and references cited therein).

Replacing the chlorido ligand on some phosphine gold(I) complexes by 1-thio-β-D-glucose tetraacetate was reported to result in an enhancement of both the cytotoxic effects and uptake [16].

Thus, we decided to substitute the chlorido ligand of **2** by both thio-β-D-glucose tetraacetate and thio-β-D-glucose (Scheme 1). While the tetraacetate derivative **3** was obtained by deprotonation of the thiol using 1 M NaOH in acetone [20], the thio-β-D-glucose complex **4** was synthesized by direct reaction of the commercially available sodium thiolate-β-D-glucose with the chlorido gold carbene **2**. All compounds were fully characterized by ^{1}H and $^{13}C\{^{1}H\}$ NMR, IR, high-resolution MS and their purity was checked by elemental analysis. A far infrared spectrum confirmed the formation of an S-Au bond in both cases, displaying a novel absorption band around 370 cm^{-1} and the absence of the band at 330 cm^{-1} corresponding to the ν_{Au-Cl} stretching [21]. The ^{1}H NMR spectra of **3** and **4** show the expected 1/1 ratio of the signals of the NHC with respect to the sugar moiety. The signal of the carbenic carbon in the $^{13}C\{^{1}H\}$ NMR spectrum of **3** resonates downfield from 2 (Dd = -3.6 ppm) and is not observed in case of **4**. However, by 1H-13C correlation NMR spectroscopy, we observe a correlation spot between both the N-methyl and the methylene bridge signals in the 1H spectrum and a signal at around 181 ppm in the $^{13}C\{^{1}H\}$ spectrum of **4** (see ^{1}H-^{13}C HMBC spectrum in the Supplementary Material, Figure S1). Noteworthy, the elemental analysis of **4** shows that it is in the form of adduct with one equivalent of NaCl, probably through the hydroxyl groups of the glucose moiety as already reported for different sugars [22]. The photophysical characterization was performed for the four compounds (see details of the study in the Supplementary Material). No significant change was observed between the imidazolium salt **1** and the Au(I) NHC complexes **2-4**. The compounds display a maximum of absorption around 325 nm, a maximum of emission around 400 nm, and the molar absorption coefficient remains almost the same for the different compounds. The quantum yields are low, maybe due to a photoinduced electron transfer (PET) between the coumarin and the imidazolium/carbine [23, 24].

1.2.2. In vitro cell viability assays

The antiproliferative properties of the imidazolium salt **1** and the Au(I) NHC complexes **2-4** (with cisplatin used as comparison) were assessed by monitoring their ability to inhibit cell growth using the classical MTT assay in human ovarian cancer A2780 cell line, in human mammary carcinoma MCF7 cells, as well as in the human lung cancer A549 cell line. In addition, in order to evaluate the compounds' selectivity for cancerous compared to healthy cells, these coumarin derivatives were also tested in human embryonic kidney HEK-293T cells. Overall, the compounds are markedly less effective in all the selected cell lines in comparison to cisplatin. Only in the case of the MCF7 cells, compound **3** shows a better activity (IC_{50} = 11.6 ± 0.8 µM) than cisplatin. Notably, **3**, bearing the 1 thio-β-D-glucose tetraacetate ligand, is also the most active of the series in A2780 and MCF7 cells, as well as the one relatively selective for cancer cells with

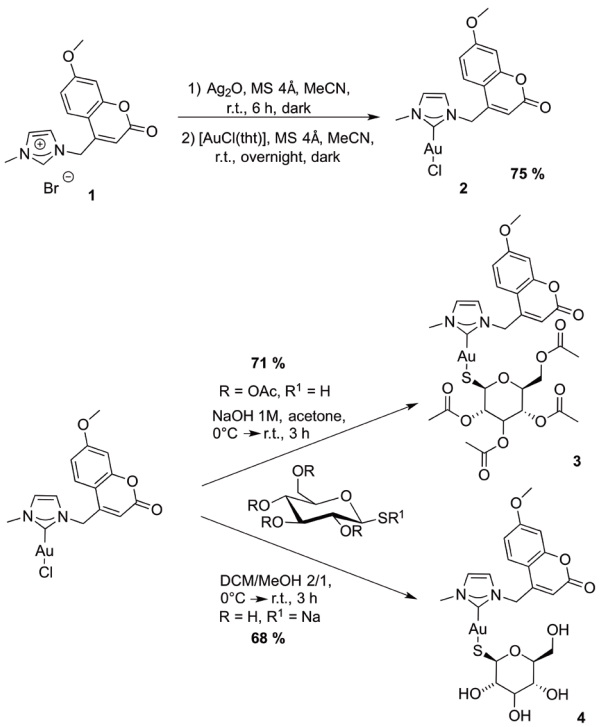

Scheme 1. Synthesis of the investigated gold(I) NHC complexes.

respect to non-cancerous ones. The inactivity of 4 in all tested cells, rules out the idea that the 1 thio-β-D-glucose ligand may enhance the compound's uptake via GLUT-1 transporters.

Table 1. Effects of compounds **1-4** on cell viability in human ovarian carcinoma A2780 cells, in human lung cancer A549 cells, in human mammary carcinoma MCF7 cells, and in embryonic kidney cells (HEK-293T) after 72 h incubation

	IC_{50} (μM) [a]			
Compound	**A2780**	**A549**	**MCF7**	**HEK-293T**
1	46.9 ± 13.3	52.5 ± 17.9	71.2 ± 5.2	>100
2	45.5 ± 7.5	95.8 ± 5.3	39.7 ± 11.8	48.0 ± 8.4
3	11.6 ± 0.8	55.6 ± 12.6	12.9 ± 3.8	15.2 ± 1.7
4	>100	>100	64.5 ± 11.5	>100
Cisplatin	1.9 ± 0.6	8.0 ± 0.5	20.0 ± 3.1	11.0 ± 2.9

[a] Values are the mean ± SE of at least three determinations.

Because TrxR is a potential target for gold compounds, *in vitro* inhibition of rat TrxR by **1-4** was studied using an established protocol. The results summarized in Figure 1 and Table 2 show that the gold(I) NHC complexes inhibit both TrxR1 and TrxR2, although less efficiently than the gold(I) compound auranofin. Notably, ligand **1** is ineffective as inhibitor at least until 30 μM concentration (Table 2). Moreover, the new complexes are much less efficient with respect to both the closely related selenium enzyme glutathione peroxidase (Gpx), and the Se-free glutathione reductase (GR) having IC_{50} values >10000 nM. Notably, minor Gpx inhibition was shown for different gold(I) NHC complexes previously reported [25].

Additional complementary information on the interaction of TrxR with compound **1-3**, and possible binding sites was obtained through the application of a specific biochemical assay relying on the thiol-tagging reagent BIAM (biotin-conjugate iodoacetamide). BIAM selectively alkylates TrxR in a pH dependent manner; at pH 6.0 only seleno-cysteines and low pK_a cysteines are alkylated. In our experiments, TrxR1 was treated with metal complex, and afterwards, sample aliquots were treated with BIAM at pH 6.0. Thus, the samples were analysed by SDS-PAGE. BIAM-labelled proteins were detected with horseradish peroxidase-conjugated streptavidin (see Figure S3 and Experimental Section for further details). The immunoblotting indicated that the tested gold complexes are able to target, although to slightly varying extents, the seleno-cysteine residues

Table 2. IC_{50} values for TrxRs, GR and Gpx inhibition calculated for compounds **1-4**.

	IC_{50} (nM) [a]			
Compound	**A2780**	**A549**	**MCF7**	**HEK-293T**
1	>10000	>10000	>10000	>10000
2	16.38 ± 1.32	76.52 ± 3.2	>1000	>500
3	17.90 ± 1.8	78.66 ± 1.2	>1000	>500
4	6.49 ± 0.2	54.02 ± 1.3	>1000	>1000
Auranofin	1.5 ± 0.2	24.3 ± 1.2	>1000	>1000

[a] Values are the mean ± SE of at least three determinations.

present in the enzyme redox-active motif.

To assess whether TrxR inhibition by the compounds under study could contribute to the observed antiproliferative effects on cells, enzyme activity was also evaluated on protein extracts obtained from A2780 cells, pre-treated with 10 μM of the compound **3** (close to the IC_{50} for the antiproliferative effects) for 48 h. In this case we observed an inhibition of thioredoxin reductase activity of ca. 30% with respect to control samples (Figure S4 in the supplementary material). Conversely glutathione reductase, tested in the same cell lysates, appears to be largely stimulated. This fact can be explained as a response to the stress that cells are subjected to after inhibition of the thioredoxin system. In fact, as a control, isolated GR is not inhibited by this compound.

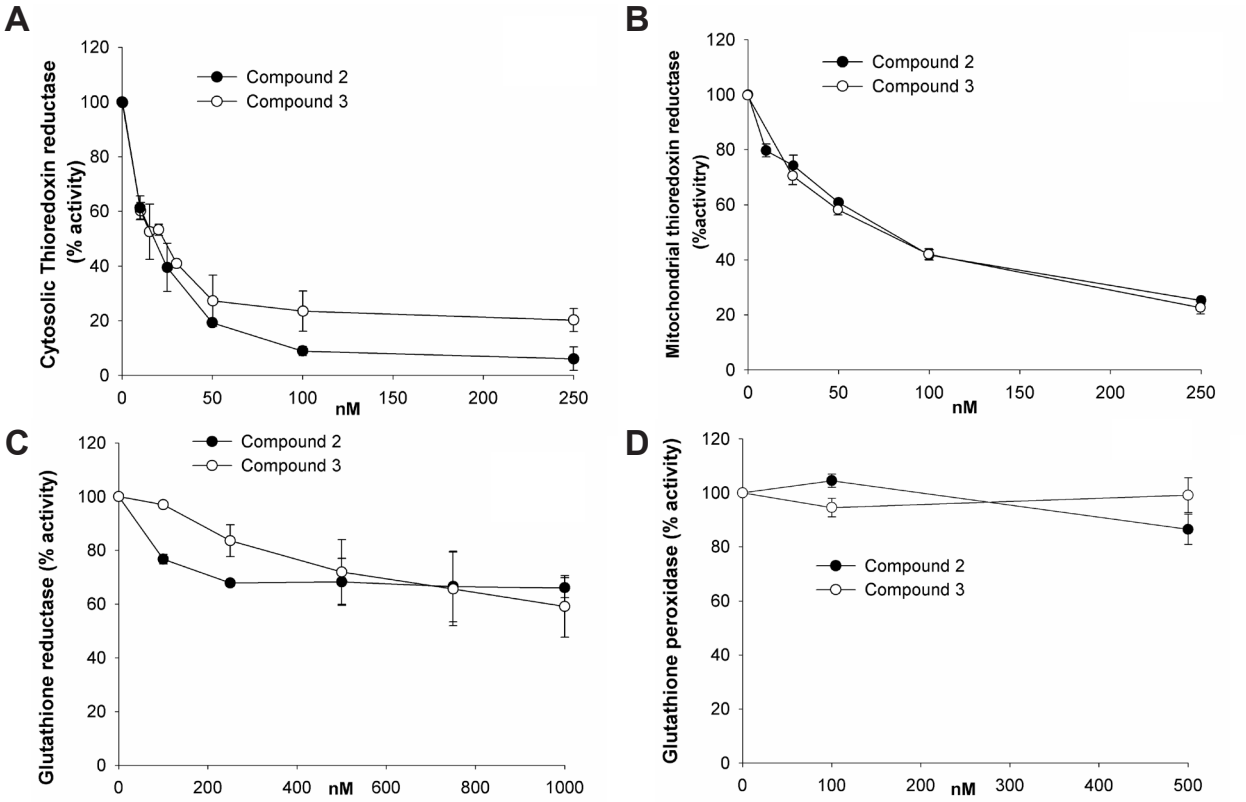

Figure 1. Effect of compounds **2-3** on cytosolic (A) and mitochondrial (B) TrxRs, (C) GR and (D) Gpx enzymes. The compounds were tested in isolated and purified enzymes.

B1

1.2.3. Fluorescence microscopy

It is worth mentioning that, among the various strategies to achieve metal compounds imaging in biological environments, fluorescence microscopy is certainly one of the most explored, and an increasing number of publications has appeared reporting on bifunctional metal compounds bearing fluorescent moieties for both therapeutic and imaging applications [26, 27]. Thus, recently, we described a gold(I) NHC complex bearing a fluorescent anthracenyl ligand whose cytotoxic effects were investigated *in vitro* in different lines of normal and cancerous human cells [28].

Similarly, the uptake of **3** was evaluated in A2780 cells by using fluorescence confocal microscopy. Figure 2 shows typical fluorescence images of cells treated with 3 (50 μM) for 2 h at 37 °C. Unfortunately, the low fluorescence of the compounds allowed visualization only at 50 μM or higher. We avoided longer incubation times due to the relatively high tested concentrations of compounds, which may have induced rapid cell death. In the obtained images, preserved cell morphology confirms viability after treatment, and compound's uptake is evident, as well as its accumulation in the nuclei (colocalization with PI staining).

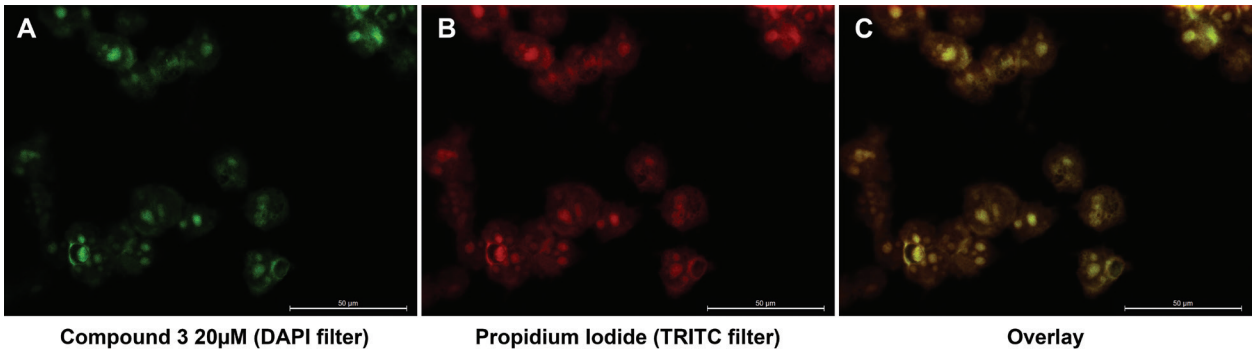

Figure 2. Visualization of gold(I)–NHC compound using confocal microscopy. A2780 cells were incubated for 2 h with 50 µM of 3 at 37 °C. A: fluorescence of the compound; B: propidium iodide localization; C: merge.

1.3. Conclusions

In summary, we have synthesized and characterized a new family of gold(I) NHC complexes bearing a fluorescent coumarin-type carbene ligand, using a limited number of steps (2-3). Two of the reported compounds bear thio-*β*-D-glucose groups as second ligand. Notably, this study was initiated in the frame of ongoing studies in our laboratories aiming at developing new organometallic gold compounds as anticancer agents. In fact, as demonstrated by numerous studies, regulating the reactivity of gold compounds *via* the optimization of an appropriate organometallic scaffold may constitute a strategy to achieve selectivity for cancer tissues, a feature that is often lacking with other types of coordination gold complexes.

Thus, the new compounds have been tested in different cancer cell lines showing moderate antipoliferative properties, in particular the derivative bearing the 1-thio-*β*-D-glucose tetraacetate ligand (3), which was also uptaken in cancer cells as shown by fluorescence microscopy. Preliminary mechanistic studies have demonstrated that the compounds are able to inhibit the cancer relevant enzyme thioredoxin reductase, most likely targeting the seleno-cysteine residue in the active site. Presently, further studies are ongoing in our labs to validate this protein target, since other interactions may occur between the gold(I) compounds and other relevant biomolecules. As an example, a recent study described for the first time the properties of a cationic gold(I) bis-NHC complex containing a caffeine-based ligand as DNA G-quadruplex stabilizing agent with exquisite quadruplex-over-duplex DNA selectivity [29].

1.4. Experimental Section

General Remarks: All reactions were carried out under an atmosphere of purified argon using Schlenk techniques. Solvents were dried and distilled under argon before use. The precursor [AuCl(tht)] (Uson R. et al, Inorg Synth. 1989, 26, 85-91) has been synthesized according to literature procedure. All other reagents were commercially available and used as received. All the analyses were performed at the "Plateforme d'Analyses Chimiques et de Synthèse Moléculaire de l'Université de Bourgogne". The identity and purity (≥ 95%) of the complexes were unambiguously established using high-resolution mass spectrometry, elemental analysis, NMR and IR spectrometries. Exact mass of the synthesized complexes were obtained on a Thermo LTQ Orbitrap XL. Elemental analyses were performed on a Thermo Electron Flash EA 1112 Series analyzer. ^{1}H- (300.13, 500.13 or 600.23 MHz) and 13C- (125.77 or 150.90 MHz) NMR spectra were recorded on Bruker 300 Avance III, 500 Avance III or 600 Avance II spectrometers. Chemical shifts are quoted in ppm (δ) relative to TMS (1H and 13C) using the residual protonated solvent (1H) or the deuterated solvent (^{13}C) as internal standards. Infrared spectra were recorded on a Bruker Vector 22 FT-IR spectrophotometer (Golden Gate ATR) and far infrared spectra were recorded on a Bruker Vertex 70v FT-IR spectrophotometer (ATR Diamant).

• **3-[(7-methoxy-2-oxo-2H-chromen-4-yl)methyl]-1-methylimidazolium bromide (1)**

A two-neck round-bottom flask was charged under argon with 1 g of 4 (bromomethyl) 7 methoxy-2H-chromen-2-one (3.76 mmol) which was suspended in THF (50 mL). 1-methylimidazole (0.31 mL, 3.76 mmol) was added dropwise

and the mixture was refluxed overnight. After removing of the THF under vacuum, the obtained white powder was suspended into dry dichloromethane and a large amount of diethyl ether. The suspension was filtered and the residue was dried under vacuum to afford the pure product as a white powder (1.26 g, 96 % yield).

^{1}H NMR (DMSO-d6, 300.13 MHz, 300 K): 3.88 (s, 3 H, N-Me), 3.89 (s, 3 H, O-Me), 5.78 (s, 2 H, N-CH_2), 5.89 (s, 1 H, CH^A), 7.02 (dd, 1 H, $^3J_{H-H}$ = 9.0 Hz, $^4J_{H-H}$ = 2.7 Hz, CH^C), 7.08 (d, 1 H, $^4J_{H-H}$ = 2.7 Hz, CH^B), 7.76 (d, 1 H, $^3J_{H-H}$= 9.0 Hz, CH^D), 7.80 (s, 1 H, CH^{Im}), 7.84 (s, 1 H, CH^{Im}), 9.22 (s, 1 H, N=CH-N^+).

^{13}C{1H} (DMSO-d6, 75.78 MHz, 300 K): 36.6 (s, N-CH3), 48.8 (s, N-CH2), 56.6 (s, O-CH3), 101.6 (s, CHB), 110.7 (s, CHA), 113.1 (s, CHC), 123.4 (s, CHIm), 124.7 (s, CHIm), 126.1 (s, CHD), 138.2 (s, N=CH-N+), 149.8 (s, Cquat-CHD), 155.5 (s, Cquat-OC(O)), 160.2 (s, C(O)), 163.4 (s, Cquat-OMe).

FT-IR (ATR, cm^{-1}): 3122, 3064, 2847, 1705, 1607, 1564, 1515, 1464, 1439, 1400, 1342, 1286, 1270, 1211, 1169, 1137.

ESI-MS (DCM/MeOH), positive mode exact mass for $C_{15}H_{15}N_2O_3^+$ (271.10772): measured *m/z* 271.10664 $[M\ Br]^+$.

Anal. Calc. for $C_{15}H_{15}N_2O_3Br$: C, 51.30, H, 4.31, N, 7.98 %. Found: C, 51.27, H, 4.05, N, 8.03 %.

• 3-[(7-methoxy-2-oxo-2H-chromen-4-yl)methyl]-1-methylimidazol-2-ylidene gold(I) chloride (2)

A round-bottom flask was charged with **1** (200 mg, 0.57 mmol) and Ag_2O (106 mg, 0.46 mmol) which were suspended in dichloromethane (150 mL). The mixture was reacted for 6 h at room temperature in the dark. [AuCl(tht)] (182 mg, 0.57 mmol) was then added and the reaction was stirred overnight at room temperature in the dark. After filtration through Celite, the filtrate was concentrated under reduced pressure. Upon addition of a large amount of diethyl ether, a pale yellow precipitate was formed and was collected by filtration. The residue was dried under vacuum to afford the pure product as a pale yellow powder (215 mg, 75 % yield).

^{1}H NMR ($CDCl_3$, 300.13 MHz, 300 K): 3.89 (s, 3 H, N-Me), 3.92 (s, 3 H, O-Me), 5.55 (s, 2 H, N CH_2), 5.68 (s, 1 H, CH^A), 6.85 (d, 1 H, $^4J_{H-H}$ = 2.7 Hz, CH^B), 6.89 (dd, 1 H, $^3J_{H-H}$ = 9.0 Hz, $^4J_{H-H}$ = 2.7 Hz, CH^C), 7.00 (d, 1 H, $^3J_{H-H}$ = 1.8 Hz, CH^{Im}), 7.06 (s, 1 H, $^3J_{H-H}$ = 1.8 Hz, CH^{Im}), 7.52 (d, 1 H, $^3J_{H-H}$ = 9.0 Hz, CH^D).

^{13}C{1H} ($CDCl_3$, 75.78 MHz, 300 K): 38.6 (s, N-CH_3), 51.1 (s, N-CH_2), 55.9 (s, O-CH_3), 101.5 (s, CHB), 110.3 (s, CH^A), 110.8 (s, C_{quat}-CH_2), 112.9 (s, CH^C), 120.9 (s, CH^{Im}), 122.9 (s, CH^{Im}), 124.5 (s, CH^D), 148.8 (s, C_{quat}-CH^D), 155.6 (s, C_{quat}-OC(O)), 160.2 (s, C(O)), 163.4 (s, C_{quat}-OMe), 173.5 (s, $C_{carbene}$).

FT-IR (ATR, cm^{-1}): 3129, 2943, 1709, 1610, 1558, 1515, 1465, 1429, 1397, 1348, 1331, 1288, 1245, 1207, 330.

ESI-MS (DCM/MeOH), positive mode exact mass for $C_{15}H_{15}N_2O_3AuClNa^+$ (525.02507): measured *m/z* 525.02328 $[M+Na]^+$.

Anal. Calc. for $C_{15}H_{15}N_2O_3AuCl$: C, 35.84, H, 2.81, N, 5.57 %. Found: C, 35.74, H, 3.00, N, 5.50 %.

• 3-[(7-methoxy-2-oxo-2H-chromen-4-yl)methyl]-1-methylimidazol-2-ylidene gold(I) (thio-β-D-glucose tetraacetate) (3)

A Schlenk tube was charged under argon with thio-*β*-D-glucose tetraacetate (36 mg, 0.10 mmol) which was dissolved in degassed acetone (3 mL). 1 M NaOH (0.1 mL, 0.10 mmol, 1 eq.) was added and the mixture was stirred for 30 min at room temperature. The mixture was then transferred onto a solution of 1 (50 mg, 0.10 mmol) in 5 mL of degassed acetone at 0°C. At the end of the addition, the ice bath was withdrawn and the mixture was stirred for 3 h at room temperature in the dark. The solvent was removed under vacuum. Dichloromethane was added and the mixture was filtered through Celite. The filtrate was concentrated under reduced pressure. An off-white precipitate was formed after addition of a large amount of n-pentane. The precipitate was filtered and dried under vacuum to give the pure product as an off-white powder (58 mg, 71 % yield).

^{1}H NMR ($CDCl_3$, 300.13 MHz, 300 K): 1.95 (s, 3 H, CH_3-COO), 2.00 (s, 3 H, CH_3-COO), 2.02 (s, 6 H, 2 CH_3-COO), 3.67-3.72 (m, 1 H, CH_{sugar}), 3.87 (s, 3 H, N-Me), 3.95 (s, 3 H, O-Me), 4.06 (dd, 1 H, $^2J_{H-H}$ = 12.3 Hz, $^3J_{H-H}$ = 2.4 Hz, $CH_{A-B,sugar}$), 4.20 (dd, 1 H, $^2J_{H-H}$ = 12.3 Hz, $^3J_{H-H}$ = 4.8 Hz, $CH_{A-B,sugar}$), 4.99-5.11 (m, 4 H, 4 CH_{sugar}), 5.57 (dd, 1 H, $^2J_{H-H}$ = 16.8 Hz, $^3J_{H-H}$ = 1.2 Hz, CH_{A-B}-N), 5.67 (d, 1 H, $^2J_{H-H}$ = 16.8 Hz, CH_{A-B}-N), 5.75 (s, 1 H, CH^A), 6.86 (d, 1 H, $^4J_{H-H}$ = 2.4 Hz, CH^B), 6.92 (dd, 1 H, $^3J_{H-H}$ = 8.7 Hz, $^4J_{H-H}$ = 2.4 Hz, CH^C), 6.96 (d, 1 H, $^3J_{H-H}$= 1.8 Hz, CH^{Im}), 7.03 (d, 1 H, $^3J_{H-H}$ = 1.8 Hz, CH^{Im}), 7.67 (d, 1 H, $^3J_{H-H}$ = 8.7 Hz, CH^D).

^{13}C{1H} ($CDCl_3$, 125.77 MHz, 300 K): 20.6 (s, CH_3-COO), 20.7 (s, CH_3-COO), 20.8 (s, CH_3-COO), 21.2 (s, CH_3-COO), 38.3 (s, CH_3-N), 50.9 (s, CH_2-N), 55.9 (s, CH_3-O), 63.0 (s, CH_2-$_{sugar}$), 69.0 (s, CH_{sugar}), 74.3 (s, CH_{sugar}), 75.8 (s, CH_{sugar}), 77.6 (s, CH_{sugar}), 83.1 (s, CH_{sugar}), 101.4 (s, CH^B), 110.6 (s, C_{quat}-CH2), 111.0 (s, CH^A), 112.9 (s, CH^C), 120.7 (s, CH^{Im}), 122.8 (s, CH^{Im}), 125.0 (s, CH^D), 149.3 (s, C_{quat}-CH^D), 155.6 (s, C_{quat}-OC(O)), 160.4 (s, C(O)coum.), 163.3 (s,

C_{quat}-OMe), 169.6 (s, $C(O)_{sugar}$), 169.9 (s, Ccarbene), 170.2 (s, $C(O)_{sugar}$), 170.7 (s, $C(O)_{sugar}$).

FT-IR (ATR, cm^{-1}): 2946, 1735, 1613, 1561, 1463, 1430, 1368, 1288, 1219, 1147, 1031, 373.

ESI-MS ($CDCl_3$/MeOH), positive mode exact mass for $C_{29}H_{33}N_2O_{12}AuSNa^+$ (853.13119): measured *m/z* 853.12907 $[M+Na]^+$.

Anal. Calc. for $C_{29}H_{33}N_2O_{12}AuS$: C, 41.93, H, 4.00, N, 3.37, S, 3.86 %. Found: C, 41.54, H, 4.20, N, 3.27, S, 3.09 %.

• 3-[(7-methoxy-2-oxo-2H-chromen-4-yl)methyl]-1-methylimidazol-2-ylidene gold(I) (thiolato-β-D-glucose) (4)

A flame-dried Schlenk tube was charged under argon with sodium thiolate-*β*-D-glucose (26 mg, 0.12 mmol) which was suspended in methanol (3 mL). This mixture was transferred onto a solution of 2 (60 mg, 0.12 mmol) in 6 mL of dichloromethane at 0°C. After the end of the addition, the ice bath was withdrawn and the mixture was stirred for 3 h at room temperature. The solution was filtered under argon through Celite using a flame-dried sintered glass. Upon concentration under reduced pressure, and addition of a large amount of a mix diethylether/n pentane, a white precipitate was formed. The precipitate was filtered and dried under vacuum to afford the product as an adduct with one equivalent of NaCl (58 mg, 68 % yield).

^{1}H NMR (DMSO-d6, 600.23 MHz, 300 K): 2.50 (dt, 1 H, $^3J_{H-H}$ = 9.0 Hz, $^3J_{H-H}$ = 3.6 Hz, CH_{sugar}), 2.93-3.04 (m, 3 H, 3 CH_{sugar}), 3.24-3.28 (m, 1 H, CH_2-sugar), 3.55 (ddd, 1 H, $^2J_{H-H}$ = 11.4 Hz, $^3J_{H-H}$ = 5.4 Hz, $^3J_{H-H}$ = 1.8 Hz, CH_{sugar}), 3.82 (s, 3 H, NCH_3), 3.87 (s, 3 H, OCH_3), 3.97 (broad s, 1 H, OH), 4.35 (pseudo t, 1 H, $^3J_{H-H}$ = 5.7 Hz, CH_2-OH), 4.47 (d, 1 H, $^3J_{H-H}$ = 9.0 Hz, CH_{sugar}), 4.71-4.73 (m, 2 H, 2 OH), 5.59 (s, 1 H, CH^A), 5.64 (s, 2 H, NCH_2), 7.01 (dd, 1 H, J_{H-H}= 8.4 Hz, $^4J_{H-H}$= 1.8 Hz, CH^C), 7.05 (s, 1 H, CH^B), 7.52 (s, 2 H, 2 CH^{Im}), 7.86 (d, 1 H, $^3J_{H-H}$ = 8.4 Hz, CH^D).

^{13}C{1H} NMR (DMSO-d6, 125.77 MHz, 300 K): 37.5 (broad s, NCH_3), 49.9 (broad s, NCH_2), 56.0 (s, OCH_3), 61.4 (s, CH_2-sugar), 70.5 (s, CH_{sugar}), 77.4 (s, CH_{sugar}), 80.1 (s, CH_{sugar}), 81.1 (s, CH_{sugar}), 85.1 (s, CH_{sugar}), 101.2 (s, CH^B), 109.3 (broad s, C_{quat}-CH_2), 110.5 (s, CH^A), 112.4 (s, CH^A), 121.9 (broad s, CH^{Im}), 123.3 (broad s, CH^{Im}), 125.8 (s, CH^D), 151.5 (s, C_{quat}-CH^D), 154.9 (s, C_{quat}-OC(O)), 159.8 (s, C(O)), 162.8 (s, C_{quat}-OMe), ca. 171 (Ccarbene not directly observed, see below).

FT-IR (ATR, cm^{-1}): 3365, 2909, 1710, 1610, 1559, 1515, 1463, 1399, 1349, 1289, 1146, 1020, 840, 558, 179, 171.

ESI-MS (MeOH), positive mode exact mass for $C_{21}H_{25}N_2O_8AuSNa^+$ (685.08893): measured *m/z* 685.08564 $[M+Na]^+$, ESI-MS (MeOH), negative mode exact mass for $C_{21}H_{25}N_2O_8AuSCl^-$ (697.06802): measured *m/z* 697.07103 $[M+Cl]^-$.

Anal. Calc. for $C_{21}H_{25}N_2O_8AuS.NaCl$: C, 34.99, H, 3.50, N, 3.89, S, 4.45 %. Found: C, 34.38, H, 3.64, N, 4.08, S, 3.21 %.

Remark: ^{13}C{^{1}H} NMR signals of 4 corresponding to the carbons of the imidazole ring appeared very broad and no signal of the carbenic carbon appeared. However, by ^{1}H-^{13}C HMBC correlation NMR spectroscopy, we could observe a correlation spot between both the N-methyl and the methylene bridge signals in the ^{1}H spectrum and a signal at around 181 ppm in the ^{13}C{1H} spectrum.

Fluorescence measurements: The steady-state fluorescence emission and excitation spectra were obtained by using a JASCO FP8560 spectrofluorometer instrument. All fluorescence spectra were corrected for instrument response. The fluorescence quantum yield (Φ_F) was calculated from equation 1.

$$\frac{\Phi_F}{\Phi_{FR}} = \frac{n^2}{n_R^2} \times \frac{\int_0^\infty I_F(\lambda_E,\lambda_F)d\lambda_F}{\int_0^\infty I_{FR}(\lambda_E,\lambda_F)d\lambda_F} \times \frac{1-10^{-A_R(\lambda_E)}}{1-10^{-A(\lambda_E)}}$$

Equation 1

Φ_F and Φ_{FR} are fluorescence quantum yields of the compound and the reference respectively. $A(\lambda_E)$ and $AR(\lambda_E)$ are the absorbance at the excitation wavelength, and n is the refractive index of the medium. I_F and I_{FR} are fluorescent intensities of the compound and the reference respectively. The reference system used was 9,10-diphenylanthracene (φ = 0.955 in cyclohexane, λ_{ex} = 366 nm).3 The data are shown in Table 1. Absorption and emission spectra of compound **1** are displayed in Figure S2 (the same behaviour was observed for complexes 2, 3 and 4).

Cell viability assay: The human lung cancer cell line A549, human breast cancer MCF-7 cells and human ovarian cancer A2780 cells, (obtained from the European Centre of Cell Cultures ECACC, Salisbury, UK) were cultured in DMEM (A549, MCF-7) and RPMI (A2780) both containing GlutaMax-I supplemented with 10% FBS and 1% penicillin/streptomycin (all from Invitrogen), at 37° C in a humidified atmosphere of 95% of air and 5% CO2 (Heraeus, Germany). Non-tumoral human embryonic kidney cells HEK-293T were cultivated in DMEM medium with GlutaMax-I, 10% FBS and 1% penicillin/streptomycin, incubated in the same conditions as other cell lines. For evaluation of growth inhibition, cells were seeded in 96-well plates (Costar, Integra Biosciences, Cambridge, MA) at a

concentration of 10000 cells/well and grown for 24 h in complete medium. Solutions of the compounds were prepared by diluting a freshly prepared stock solution (10 2 M in DMSO) of the corresponding compound in aqueous media (RPMI or DMEM depending on the cell lines). The percentage of DMSO in the culture medium never exceeded 0.2%: at this concentration DMSO has no effect on the cell viability. Cisplatin (Sigma-Aldrich) stock solutions were prepared in MilliQ water. Afterwards, the intermediate dilutions of the compounds were added to the wells (200 µL) to obtain a final concentration ranging from 0 to 200 µM, and the cells were incubated for 72 h. Following 72 h drug exposure, 3 (4,5-dimethylthiazol-2-yl)-2,5-diphenyltetrazolium bromide (MTT) was added to the cells at a final concentration of 0.50 mg.ml-1 incubated for 3-4 h, then the culture medium was removed and the violet formazan dissolved in DMSO. The optical density of each well (96-well plates) was quantified in quadruplicate at 540 nm using a multi-well plate reader and the percentage of surviving cells was calculated from the ratio of absorbance between treated and untreated cells. The IC50 value was calculated as the concentration reducing the proliferation of the cells by 50% and is presented as a mean (± SE) of at least three independent experiments.

Estimation of enzyme activities inhibition *in vitro*: Highly purified cytosolic thioredoxin reductase (TrxR1) was prepared from rat liver, according to Luthman and Holmgren, (M. Luthman and A. Holmgren, Biochemistry, 1982, 21, 6628-6633) Mitochondrial thioredoxin reductase (TrxR2) was purified from isolated rat liver mitochondria following the procedure of Rigobello et al. (M. P. Rigobello and A. Bindoli, Methods Enzymol., 2010, 474, 109-122.) Thioredoxin reductases activity was determined by measuring the ability of the enzyme to directly reduce DTNB in the presence of NADPH. (M. Luthman and A. Holmgren, Biochemistry, 1982, 21, 6628-6633) Aliquots of highly purified TrxR1 (30 nM) and TrxR2 (30 nM) in 0.2 M Na, K-phosphate buffer (pH 7.4), 5 mM EDTA, 0.25 mM NADPH were pre-incubated for 5 min with the Au-NHC coumarin derivatives. Afterwards, the reaction was started with 1 mM DTNB, and monitored spectrophotometrically at 412 nm for about 10 min.

Yeast glutathione reductase was obtained from Sigma (St. Louis Mo, USA) and used without further purification. Glutathione reductase activity was measured in 0.2 M Tris HCl buffer (pH 8.1), 1 mM EDTA, and 0.25 mM NADPH after 5 min pre-incubation with the gold complexes. The assay was initiated by the addition of 1 mM GSSG and followed spectrophotometrically at 340 nm.

Glutathione peroxidase activity was performed by the following procedure: (X Liu, K E Pietsch, S J Sturla, Chem. Res. Toxicol., 24 (2011) 726–736) aliquots of GPx from bovine erythrocytes (0.02 U) were incubated with gold compounds in a total volume of 0.5 mL of 50 mM Hepes buffer (pH 7.0) containing 3 mM EDTA and 0.3 mM NADPH at 25°C. After 5min, 4 mM GSH and 25 nM glutathione reductase were added. After 2 min of incubation the reaction was started by the addition of 200 µM tert-butyl hydroperoxide and monitored spectrophotometrically at 340 nm as decrease of NADPH.

BIAM assay: TrxR (1 µM) pre-reduced in presence of NADPH was incubated with different concentrations of complexes for 30 min at room temperature, in 20mM Tris-HCl buffer (pH 7.4) containing 200 µM NADPH, and 1 mM EDTA. After incubation, 8 µL of the reaction mixture was removed and added to 50 µM biotinylated iodoacetamide (BIAM) in 0.1 M Hepes- Tris pH 6.0.(J. Fang and A. Holmgren J. Am. Chem. Soc., 2006, 128 (6), pp 1879–1885) Samples were incubated at room temperature for additional 30 min to alkylate the remaining SH groups in the enzyme. Then, BIAM-modified enzyme was mixed with loading buffer and the mixture was subjected to sodium dodecyl sulfate–polyacrylamide gel electrophoresis (SDS–PAGE) on a 7.5 % gel, and the separated proteins were transferred to a nitrocellulose membrane. Proteins labelled with BIAM were detected with horseradish peroxidase-conjugated streptavidin and enhanced chemiluminescence detection.

Determination of TrxR and GR activities in cell lysates: A2780 cells (1x106) were incubated for 48 h with 10 µM of compounds 1-4, with refresh at 24 h. After incubation, cells were harvested and washed twice with ice-cold PBS. Each sample was lysed with a modified RIPA buffer. After 40 min of incubation at 0 °C, lysates were centrifuged at 14000 x g for 5 min. The obtained supernatants were tested for enzyme activities. Aliquots (50 µg) of lysates were subjected to thioredoxin reductase determination in a final volume of 250 µl of 0.2 M Na, K-phosphate buffer (pH 7.4), 5 mM EDTA, and 2 mM DTNB. After 2 min the reaction was started with 0.3 mM NADPH. In cell lysates glutathione reductase activity was also estimated using 50 µg protein/ml as reported above.

Fluorescence microscopy: Cells (A2780) were seeded (5 x 105 for each sample) and grown on 8 well microscope plates, coated with Poly-L-Lysine hydrobromide (Sigma-Aldrich, P6516) with a complete medium. After 24 h, cells were incubated with various concentrations of the complexes in RPMI, without FCS for 2 h at 37 °C and 4°C. At the end of incubation, cells were rapidly washed with cold PBS and then fixed with 2% paraformaldehyde for 30 min at 4°C. For the visualization of PI, cells were permeabilized with 0.2% Triton X-100 for 20 min at 4°C and treated with 1µg/µl of PI for 10 min at room temperature. Cells were washed once with PBS and then analyzed by confocal microscopy. As preparation for visualization, the plate wells were removed and glycerol was used to cover the slide with a glass cover slip. The fluorescence was analysed using a Leica DM4000 B Automated Upright Microscope, equipped with the appropriate filters. PI was excited at 547 nm (emission wavelength 572 nm) and the compounds at 358 nm (emission

wavelength 461 nm, DAPI filter). The acquired images were obtained using individual filters and a combined image, overlaying the fluorescence acquired with the two filters, was obtained using the Leica microscope software.

References

[1] S. Komeda, A. Casini, Curr Top Med Chem, 12 (2012) 219-235.
[2] L.E. Wedlock, S.J. Berners-Price, Aust. J. Chem., 64 (2011) 692-704.
[3] E.M. Nagy, L. Ronconi, C. Nardon, D. Fregona, Mini-Rev Med Chem, 12 (2012) 1216-1229.
[4] L. Messori, A. Casini, Curr Top Med Chem, 11 (2011) 2647-2660.
[5] A. de Almeida, B.L. Oliveira, J.D.G. Correia, G. Soveral, A. Casini, Coord Chem Rev, 257 (2013) 2689-2704.
[6] L. Ronconi, D. Fregona, Dalton Trans., (2009) 10670-10680.
[7] A. Casini, C. Hartinger, C. Gabbiani, E. Mini, P.J. Dyson, B.K. Keppler, L. Messori, J. Inorg. Biochem., 102 (2008) 564-575.
[8] J.L. Hickey, R.A. Ruhayel, P.J. Barnard, M.V. Baker, S.J. Berners-Price, A. Filipovska, J. Am. Chem. Soc., 130 (2008) 12570-12571.
[9] A. Bindoli, M.P. Rigobello, G. Scutari, C. Gabbiani, A. Casini, L. Messori, Coord. Chem. Rev., 253 (2009) 1692-1707.
[10] S.J. Berners-Price, A. Filipovska, Metallomics, 3 (2011) 863-873.
[11] Y.M. Go, D.P. Jones, Antioxid Redox Sign, 13 (2010) 489-509.
[12] J. Lu, E.H. Chew, A. Holmgren, Proc. Natl. Acad. Sci. U. S. A., 104 (2007) 12288-12293.
[13] B. Bertrand, A. Casini, Dalton Trans, 43 (2014) 4209-4219.
[14] L. Oehninger, R. Rubbiani, I. Ott, Dalton Trans, 42 (2013) 3269-3284.
[15] E. Schuh, C. Pfluger, A. Citta, A. Folda, M.P. Rigobello, A. Bindoli, A. Casini, F. Mohr, J. Med. Chem., 55 (2012) 5518-5528.
[16] E. Vergara, E. Cerrada, C. Clavel, A. Casini, M. Laguna, Dalton Trans., 40 (2011) 10927-10935.
[17] J. Lemke, N. Metzler-Nolte, Eur.J. Inorg.Chem., 21 (2008) 3359-3366.
[18] H.M.J. Wang, I.J.B. Lin, Organometallics, 17 (1998) 972-975.
[19] B. Bertrand, E. Bodio, P. Richard, M. Picquet, P. Le Gendre, A. Casini, J. Organomet. Chem., (2014) 10.1016/j.jorganchem.2014.1003.1020.
[20] S.S. Gunatilleke, A.M. Barrios, J. Med. Chem., 49 (2006) 3933-3937.
[21] E.A. Allen, W. Wilkinson, Spectrochim Acta a-M, A 28 (1972) 2257-2262.
[22] J.A. Rendleman Jr, Complexes of Alkali Metals and Alkaline-Earth Metals with Carbohydrates, in: L.W. Melville, R.S. Tipson (Eds.) Advances in Carbohydrate Chemistry, Academic Press, 1967, pp. 209-271.
[23] N. Saleh, Y.A. Al-Soud, W.M. Nau, Spectrochim Acta A, 71 (2008) 818-822.
[24] P. Datta, D. Sardar, P. Mitra, C. Sinha, Polyhedron, 30 (2011) 1516-1523.
[25] R. Rubbiani, S. Can, I. Kitanovic, H. Alborzinia, M. Stefanopoulou, M. Kokoschka, S. Monchgesang, W.S. Sheldrick, S. Wolfl, I. Ott, J. Med. Chem., 54 (2011) 8646-8657.
[26] S. Tasan, O. Zava, B. Bertrand, C. Bernhard, C. Goze, M. Picquet, P. Le Gendre, P. Harvey, F. Denat, A. Casini, E. Bodio, Dalton Trans., 42 (2013) 6102-6109.
[27] F. Schmitt, P. Govindaswamy, O. Zava, G. Suss-Fink, L. Juillerat-Jeanneret, B. Therrien, J. Biol. Inorg. Chem., 14 (2009) 101-109.
[28] A. Citta, E. Schuh, F. Mohr, A. Folda, M.L. Massimino, A. Bindoli, A. Casini, M.P. Rigobello, Metallomics, (2013) 1006-1015.
[29] B. Bertrand, L. Stefan, M. Pirrotta, D. Monchaud, E. Bodio, P. Richard, P. Le Gendre, E. Warmerdam, M.H. de Jager, G.M. Groothuis, M. Picquet, A. Casini, Inorg Chem, 53 (2014) 2296-2303.
[30] A. Casini, M.C. Diawara, R. Scopelliti, S.M. Zakeeruddin, M. Grätzel, P.J. Dyson, Dalton Trans, 39 (2010) 2239-2245.
[31] M.A. Cinellu, A. Zucca, S. Stoccoro, G. Minghetti, M. Manassero, M. Sansoni, Journal of the Chemical Society, Dalton Trans, (1996) 4217-4225.
[32] L.S. Hollis, S.J. Lippard, J Am Chem Soc, 105 (1983) 4293-4299.
[33] A.D. Becke, J Chem Phys, 98 (1993) 5648-5652.
[34] A.D. Becke, Physical review. A, 38 (1988) 3098-3100.
[35] R.S. Mulliken, J Chem Phys, 23 (1955) 1833-1840.
[36] D.J. Tannor, B. Marten, R. Murphy, R.A. Friesner, D. Sitkoff, A. Nicholls, B. Honig, M. Ringnalda, W.A. Goddard, J Am Chem Soc, 116 (1994) 11875-11882.
[37] A.P. Martins, A. Marrone, A. Ciancetta, A. Galán Cobo, M. Echevarría, T.F. Moura, N. Re, A. Casini, G. Soveral, PloS one, 7 (2012) e37435.
[38] D. Fu, A. Libson, R. Stroud, in: Ion Channels - from atomic resolution physiology to functional genomics, 2002, pp. 51-65.
[39] J. E. D. Glendening, K. Badenhoop, A. E. Reed, J. E. Carpenter, J. A. Bohmann, C. M. Morales, and F. Weinhold, in, Theoretical Chemistry Institute, University of Wisconsin, Madison, 2001.
[40] W.L. Jorgensen, D.S. Maxwell, J. Tirado-Rives, J Am Chem Soc, 118 (1996) 11225-11236.
[41] R.A.F. G. Kaminski, J. Tirado-Rives, W. L. Jorgensen, J. Phys. Chem. B, (2001) 6474-6487.